J Mater Sci (2009) 44:2119–2127
DOI 10.1007/s10853-009-3311-4

Nanoindentation strain rate sensitivity of thermo-oxidized PMR-15 polyimide

Y. C. Lu · G. P. Tandon · S. Putthanarat ·
G. A. Schoeppner

Received: 16 October 2008 / Accepted: 2 February 2009 / Published online: 26 February 2009

Abstract This article reports the study of rate-dependent mechanical properties of thermal-oxidized PMR-15 polyimide resins with a nanoindenter. A series of PMR-15 resin specimens have been isothermally aged at various temperatures, times, and pressures. The strain rate sensitivity of oxidized surface layer obtained at each aging condition has been determined from nanoindentation creep experiments using constant displacement-rate $(\dot{h})$ method. Results show that the average strain rate sensitivity in the oxidized surface layer is notably higher than that in the unoxidized interior, indicating that the oxidized surface layer has limited ductility and thus is susceptible to fracture. Effects of aging environments (time, temperature, and pressure) on mechanical properties are also examined. After passing the initial oxidation stage, the change in strain rate sensitivity become insignificant and less sensitive to aging parameters.

Introduction

Polymer matrix composites (PMCs) have been increasingly used in high temperature aerospace and space structures such as aircraft engines and rocket components. In those applications, the materials are exposed to high temperature and to oxygen, which lead to thermal degradation and oxidative degradation of polymer resins (graphite fiber degradation is in general negligible) [1–3]. The thermal degradation generally occurs throughout the material, thus, the changes in mechanical properties can be accessed by testing aged bulk specimens. The oxidative degradation, on the other hand, occurs only at the surfaces of the material [4–8]. During oxidation, oxygen diffuses into the surface and reacts with the polymer. As a result, a thin oxidized surface layer forms on the exposed material, the thickness of which is typically in the range of microns or less. The mechanical properties in the oxidized surface layer can be significantly different from those in the unoxidized interior, because of various physical and chemical changes occurred during oxidation.

The absence of robust methods to characterize the mechanical properties of oxidized high temperature polymer matrix composites (PMCs) has limited our ability to predict material in-service performance. Recently, the nanoindentation technique has been used to characterize the static mechanical properties of oxidized polymers, from which the elastic modulus is obtained [9–11]. Results indicate that the modulus of oxidized surface layer is generally higher than that of unoxidized interior. The measured increase in modulus in the surface oxidization layer is believed to be a manifestation of the chemical changes occurring in the polymer during oxidation. The PMR-15 network has two oxidation sensitive sites: the bridging methylene of the aromatic diamine and the aliphatic region corresponding to the polymerized nadic end cap. During oxidation, the carbonyls and acids are developed by oxygen addition and the aliphatic is transformed to unsaturated carbon [4, 5]. Those changes lead to the higher rigidity and thus the higher modulus in the oxidized layer.

The modulus number may only yield information about static, elastic behavior of oxidized materials. From material

---

Y. C. Lu (✉)
University of Kentucky, Lexington, KY, USA
e-mail: chlu@engr.uky.edu

G. P. Tandon · S. Putthanarat
University of Dayton Research Institute, Dayton, OH, USA

G. A. Schoeppner
Air Force Research Laboratory, Wright Patterson AFB, OH, USA

development point of view, it is necessary to know the rate-dependent deformation such as creep. Furthermore, the rate-dependent parameters are needed in mechanistic models to predict the damage evolution and life expectancy of the aircraft components [3, 12]. In this study, the rate-dependent deformation of thermal-oxidized polymer resin is characterized by nanoindentation strain rate sensitivity. Although macroscopic strain rate sensitivity tests have been well understood, the nanoscale strain rate sensitivity tests are still relatively new. Strain rate sensitivity experiment through nanoindentation was probably first performed by Pollock et al. [13] and then refined by Mayo et al. [14–17], Poisl et al. [18], Stone and Yoder [19], Lucas and Oliver [20]. The strain rate sensitivity experiment typically involves loading the indenter at a high loading rate and then holding the load on the indenter constant while monitoring the displacement of the indenter as a function of time. From experiments, both the hardness and the indentation strain rate are calculated. The hardness–indentation strain rate pairs are then plotted on a log–log graph to determine the strain rate sensitivity—the slope of the linear graph.

It should be also mentioned that a theoretical analysis for nanoindentation strain rate sensitivity has been recently established by Cheng and Cheng [21]. They have conducted a dimensional analysis on nanoindentation of a power-law creep solid ($\sigma = b\dot{\varepsilon}^m$, where m is the strain rate sensitivity and b a constant) and proved that hardness (H) is proportional to the indentation strain rate $\left(\dot{h}/h\right)$ by a scaling function

$$H = \left(b\prod_{\gamma}\right)\left(\frac{\dot{h}}{h}\right)^{m} \tag{1}$$

The above equation indicates that during nanoindenter creep experiment the hardness (H) will decrease with increasing indentation depth (h) and that the slope of $\ln(H)$ versus $\ln\left(\dot{h}/h\right)$ would give the strain rate sensitivity (m).

Isothermally aged PMR-15 polyimide was tested in the experiments of this study. PMR-15 was chosen, since it is the most widely used matrix material for high temperature composites used in aerospace and space industries. The oxidation mechanisms of PMR-15 have also been extensively studied in the literature [1–7, 22–25]. Thus, this material is a good system on which to study the rate-dependent deformation of oxidized polymer resin through nanoindentation method.

Experimental

Sample preparation

Rectangular PMR-15 neat resin plaques were fabricated in an autoclave using a steel die mold with Teflon coating and the manufacturer's recommended cure cycle. Subsequent to the plaque being post-cured in air for 16 h at 343 °C, it was cut using a diamond wet-saw with distilled water as a cooling medium. The sample was then washed using a common household soap and then rinsed with distilled water for a minimum of 5 min. The specimen was then dried with standard paper towels and placed in a vacuum oven at 105 °C for a minimum of 48 h to remove any moisture within the samples, and stored in a nitrogen-purged desiccator until testing. The specimen was isothermally aged at various temperatures (288, 316, and 343 °C). The aging time ranged from 1 h to over 3000 h. The aging pressures used were ambient pressure, 0.414 and 0.62 MPa.

Smaller specimens were subsequently dry-sectioned from the aged plaques using a diamond saw with distilled water as a cooling medium. The specimen was then potted in Jeffamine 828-D230 epoxy resin that was cured at room temperature for three days. The surface of the specimen was prepared by grinding papers and polishing compounds, the final polishing compound being alumina with an average particle size of 0.3 μm. These potted cross sections were used for optical microscopy and nanoindentation measurements.

Optical examination

The Nikon Microphoto-FXL, Model F84006, in the bright-field mode was used to examine the morphology of the oxidized materials. The intensity of the microscope light was adjusted such that the entire aged sample was well illuminated. Care was exercised to ensure that the potted specimen was flat once the oxidation layer was in view under the microscope. This was done by verifying that the layer is approximately of same thickness on all the sides of the specimen. If it was not, either the sample might have been cut obliquely or not mounted flat and would need to be redone. The edge of the aged specimen was then brought into focus, and the thickness of the oxidative layer and transition region were measured (The definitions of "oxidative layer" and "transition zone" are given later in section "Phenomenology of thermo-oxidization of PMR-15"). A total of 12 measurements were made, three thickness values along each edge of the specimen, and the averages were computed.

Nanoindentation strain rate sensitivity

The strain rate sensitivity tests were performed on a Nano Indenter XP (MTS NanoInstruments, Oak Ridge, TN) with a Berkovich diamond tip. The indenter has a nominal tip radius <20 nm and an inclined angle of $\theta = 65.3°$. The strain rate sensitivity was determined from nanoindentation creep experiments. In these experiments, the indenter was first brought to make contact with the sample surface and then ramped to a desired load (typically 50 mN) within 2 s, corresponding to a loading rate of 25 mN/s. Experiments with different loading rates had also been conducted. The indenter was then held at the constant load for a period of 600 s. The hold segment was followed by an unload segment. During all the experiments, the indenter load and displacement were recorded as a function of time. The thermal drift rate during the experiments was controlled to be less than 0.1 nm/s.

The instantaneous indentation hardness (H) was calculated according to the standard method [26, 27]

$$H = \frac{P}{A} \tag{2}$$

where P and A are the instantaneous indentation load and indenter-sample contact area, respectively.

The indenter–sample contact area (A) in nanoindentation experiments was calculated through a tip-area function [26, 27]. The coefficients in the tip-area function were estimated through a calibration process on standard reference materials (high-purity fused silica). In these experiments, the first two coefficients were used: $C_1 = 24.42$ and $C_2 = 712$. So the hardness was calculated by

$$H = \frac{P}{24.42h^2 + 712h} \tag{3}$$

The indentation strain rate was defined as the ratio of rate of penetration $(\dot{h})$ and depth of penetration (h), according to Mayo et al. [14–17] and Cheng and Cheng [21]

$$\dot{\varepsilon}_H = \frac{1}{h} \cdot \frac{\partial h}{\partial t} \tag{4}$$

During indentation creep test, the contact area (A) increased as the indenter penetrated the materials while the load was held constant. As a result, the indentation hardness decreased with a corresponding decrease in strain rate. This allowed the tabulation of indentation hardness–strain rate pairs. The hardness–strain rate pairs were then plotted on a log–log graph, and its slope yielded the strain rate sensitivity

$$m = \frac{\partial \ln H}{\partial \ln \dot{\varepsilon}_H} \tag{5}$$

All the creep experiments reported in this study were conducted at ambient condition. The temperature was monitored by a LabView data acquisition system through several J-type thermocouples embedded inside the testing chamber.

Results and discussion

Phenomenology of thermo-oxidization of PMR-15

The morphologies of isothermally aged PMR-15 specimens were examined with optical microscope (Nikon Microphoto-FXL, Model F84006) using a bright-field light. Figure 1a shows an optical micrograph of a PMR-15 neat resin specimen isothermally aged at 316 °C for a period of 215 h in ambient air; Fig. 1b shows an optical micrograph of a PMR-15 neat resin specimen isothermally aged at 288 °C for a period of 651 h in 0.414 MPa pressurized air. These micrographs reveal that there exist three distinct material regions, representing different levels of oxidation. They are: region I—the fully oxidized surface layer, region II—the active reaction zone (where a mix of oxidized and unoxidized polymers exist), and region III—an unoxidized interior. The thickness of the active reaction zone (region II) is rather small and can further reduce in thickness as the aging temperature increases [1–3].

The micrographs reveal that small voids have developed in the oxidized regions, particularly at longer aging time

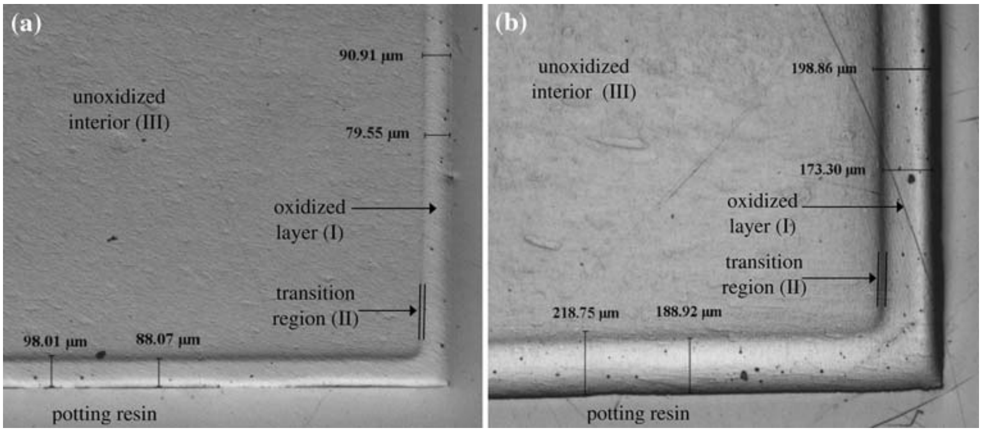

Fig. 1 Optical micrographs of oxidized PMR-15 polyimide aged at **a** 288 °C for 215 h in lab air and **b** 316 °C for 651 h in 0.414-MPa pressurized air

and higher aging pressure (Fig. 1b). The presence of voids has been explained by Meador et al. [5] using the Kirkendall effect. The Kirkendall effect refers to the migration of atoms in a solid at an interface. In the oxidation process, the inward diffusion of oxygen is slower than the outward diffusion of degradation products; therefore, the small voids form. Voids can increase in size and density over time, which act as starter points for microcracks.

The thickness of the oxidized surface has been found to depend upon the environmental conditions (time, temperature, and pressure) [1–3]. The effect of aging time on oxidized surface thickness is shown in Fig. 2 for PMR-15 aged at various temperatures (288, 316, 343 °C). Within the first hour of thermal aging, an oxidized layer of approximately 10 μm thick is seen to form on the exposed specimen surfaces. Initially, the thickness of this oxidized layer increases rapidly with aging time and then the rate of change starts to decrease. This is because the oxidation growth rate decreases with time over longer aging-time periods [1].

The oxidization rate is generally accelerated with the increase of aging temperature. Acceleration by temperature occurs by reducing the activation energy of chemical bond rupture in the polymer macromolecule. In these experiments, the specimens were all aged at relatively high temperatures: 288, 316, 343 °C (typical engine operating temperatures). Within this narrow range of temperatures, the thickness of the oxidized surface is seen to increase, but not substantially (Fig. 2).

Oxidization growth may also be accelerated by increasing the partial pressure of oxygen within the aging chamber, since the high pressure generally allows the oxygen to diffuse deeper into the interior of the specimens [1–3]. In these experiments, the PMR-15 samples were placed in a steel pressure chamber with a continuous supply of pressurized air (0.414 MPa). The pressure chamber was then put inside an air-circulating oven for elevated temperature aging. Unlike a sealed closed chamber in which the oxygen supply is depleted for long aging times, the present chamber maintains a target pressure while replenishing the air. It is seen that the elevated pressure aging of the PMR-15 resin presumably has a significant effect on the rate of diffusion of oxygen into the specimen, accelerating the oxidation process and allowing the oxygen to diffuse deeper into the interior of the specimens. This results in greater oxidation layer thicknesses than those achievable in ambient air pressure environments (Figs. 3 and 1b).

Strain rate sensitivity of unoxidized PMR-15

The nanoindentation creep tests were performed on PMR-15 resin with a Berkovich nanoindenter (a three-faced tip with a tip radius ≤20 nm). In most creep experiments, a 50 mN load was applied to the indenter tip and then maintained at this level for a length of time, typically for 600 s. The indenter displacement was recorded continuously during the test. Creep tests were first performed in the interior unoxidized regions of the aged materials to establish the experimental procedures and parameters such as effective ramping rate, holding time, etc. The mechanical properties of the interior regions are typically unchanged by the oxidation reaction and thus they remain inhomogeneous [9, 10].

Figure 4 shows the indentation hardness–time and displacement–time curves from the creep experiments

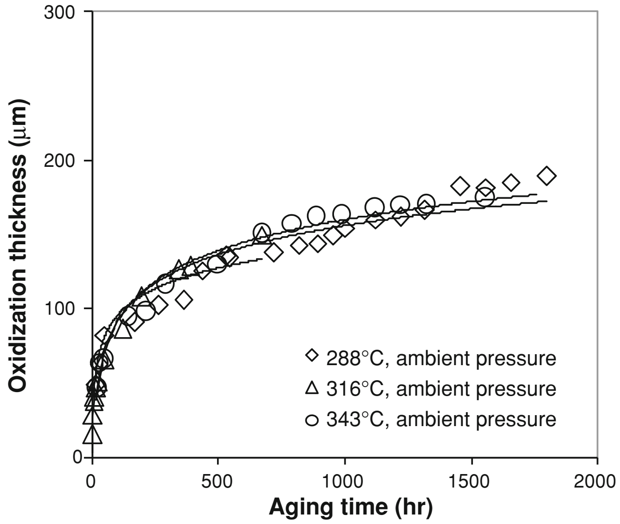

Fig. 2 Evolution of oxidized surface layer thickness as a function of aging time. Specimens are isothermally aged at 288, 316, and 343 °C

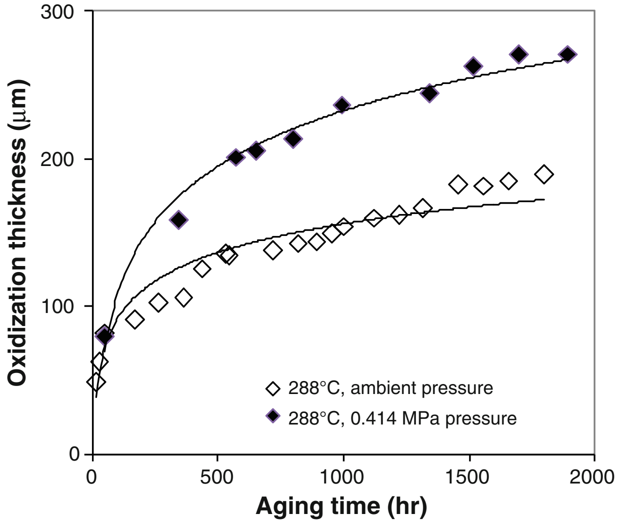

Fig. 3 Effect of aging pressure on the evolutions of oxidized surface layer thickness. Specimens are isothermally aged at 288 °C

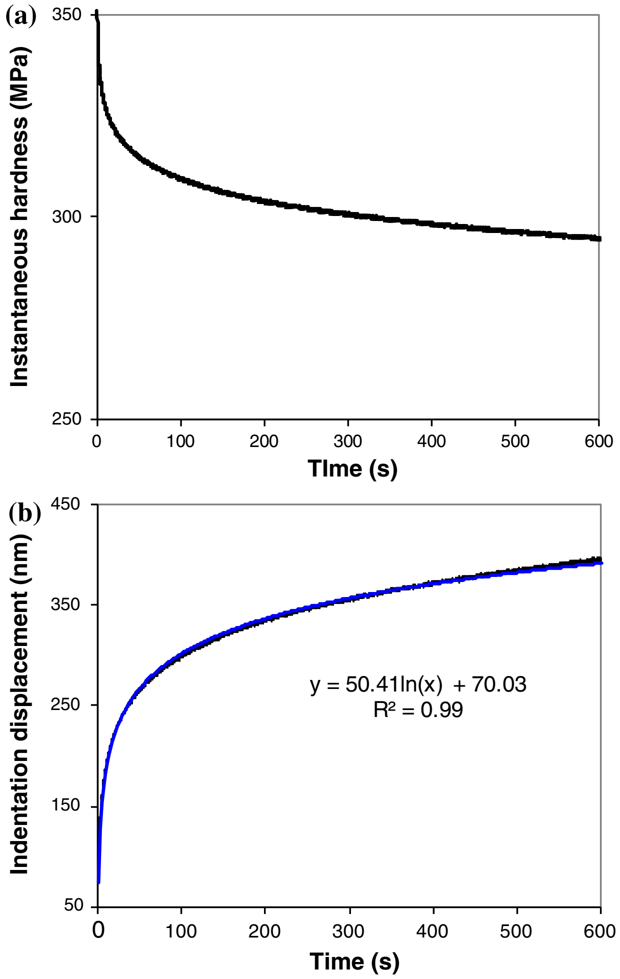

Fig. 4 The hardness–time curve (**a**) and the displacement–time curve (**b**) measured in the unoxidized interior of a PMR-15 specimen aged at 288 °C

performed in the interior region of an aged PMR-15 specimen (288 °C for 2635 h). The instantaneous hardness (H) was calculated by dividing the load (P) by the contact area (A) (Eq. 3). As expected, the hardness decreases over time since the contact area increases with continuous penetration of the indenter. The measured displacement response is smooth; no sign of influence of thermal drift. The displacement–time curve was fitted with a logarithmic function (Fig. 4b), the time derivative of which gave the indentation velocity $\left(\dot{h}\right)$. The ratio of $\dot{h}$ and instantaneous indentation depth, h, yielded the indentation strain rate, $\dot{\varepsilon}_H$. After the hardness and strain rate were obtained at each depth, they were plotted in the form of $\ln(H)$ versus $\ln(\dot{\varepsilon}_H)$, as seen in Fig. 5. It is seen that, at large displacement (corresponding to steady-state creep), the relation between hardness and strain rate is linear (the coefficient of correlation $\gg$0.99). From this plot, the strain rate sensitivity is computed. For the unoxidized PMR-15 resin, $m \approx 0.0172$.

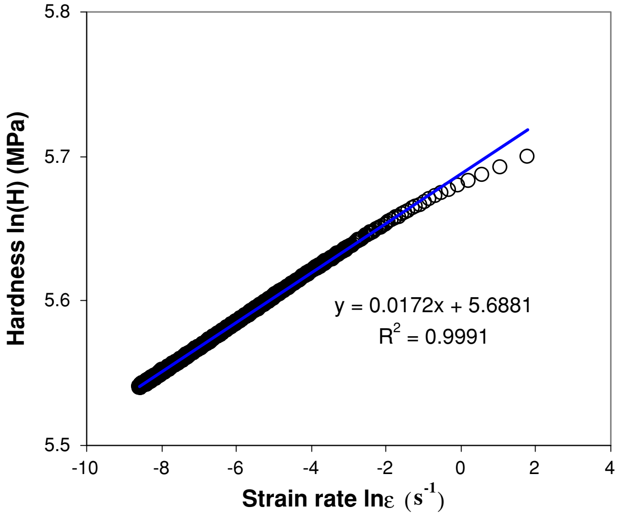

Fig. 5 The $\ln(H) - \ln(\dot{\varepsilon}_H)$ plot used to calculate the strain rate sensitivity, m, of the unoxidized PMR-15 polyimide aged at 288 °C

The strain rate sensitivity does not seem to depend upon the ramping rate of the indenter. Different ramping rates have been tried on unoxidized PMR-15 specimens. In the experiments, the indenter was loaded to 110 mN using different loading times of 0.1, 0.5, 1, 2, 5, 10, and 30 s (Fig. 6a). It is seen that the initial creep responses are different with different loading rates. After the load limit is reached, the creep responses seem to be identical (Fig. 6b). The resultant strain rate sensitivities are shown in Fig. 7. It is seen that the strain rate sensitivity is not significantly affected by the ramping rate in these nanoindentation creep experiments. Similar finding has been reported by Poisl et al. [18], by testing amorphous selenium using a similar nanoindenter.

When performing the creep experiment with an indenter, particularly with a nano-size indenter, it is often advantageous to use a fast descent rate of the indenter to ensure a much greater amount of creep during the constant-load hold. In this way, the time required for a material to reach the steady-state stage can be minimized and the creep test can be completed in a timely manner. This procedure would be particularly useful when performing creep experiments at elevated temperatures, where the thermal drift becomes a factor. However, a too fast loading rate may result in an error in load/displacement control. There is a time lag in the analog feedback loop used for controlling the indenter load or displacement. Too short loading time may lead to an overshoot of load or displacement. As seen in Fig. 6a, a load overshoot is clearly evidenced when a 0.5-s loading time was used. To avoid such an error, a moderate loading time ($t = 2$ s) was used for most of the creep experiments.

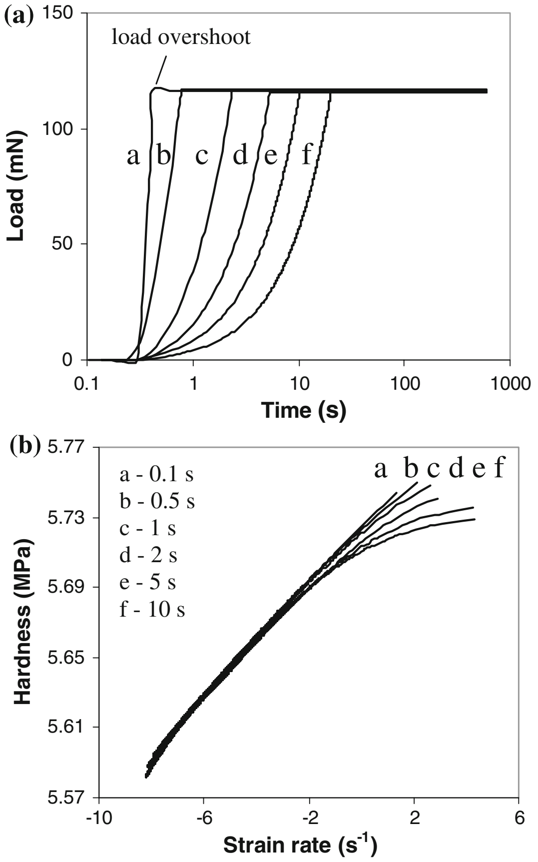

Fig. 6 Effect of loading time on indentation strain rate sensitivity measurements of PMR-15. **a** The load–time curves at different loading times and **b** the hardness–strain rate curves at different loading times

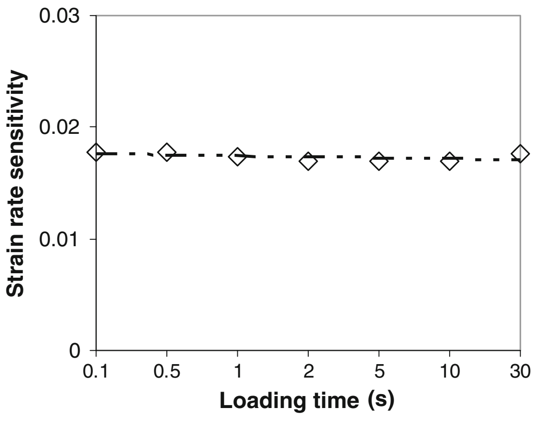

Fig. 7 Effect of loading time on nanoindentation strain rate sensitivity. The material used in these experiments was the unoxidized PMR-15 resin aged at 288 °C

Spatial variability of strain rate sensitivity of thermal-oxidized PMR-15

Optical examinations have shown that during oxidation a distinctive oxidized layer and a transition zone form on the exposed specimen. It is thus expected that the mechanical properties of the specimen would be inhomogeneous. Nanoindentation tests were performed on the cross sections of oxidized PMR-15 resins (Fig. 1a, b) to examine the spatial variability of their mechanical properties. By indenting exclusively the thin surface layer, the mechanical properties of oxidized material can be precisely measured. The mechanical properties of the unoxidized material are obtained by indenting the interior regions of the aged specimens.

The spatial variability of strain rate sensitivity of PMR-15 was investigated by a "scan-indentation" technique. The scan-indentation is a series of indentation across the oxidized surface layer and the unoxidized interior, as illustrated in Figs. 8a and 9a. Enough distance was given between indentations to minimize the effect of residual stress from previous indentation. Specimens used were aged at 288 °C in 0.414-MPa pressurized air for 651 and 1518 h. On each specimen, the scan was first performed from the oxidized edge towards the unoxidized central region (starting from point A to B), and then from the central region toward the edge (starting from point A′ to B′).

The strain rate sensitivity results are shown in Figs. 8b and 9b, where the respective transition thickness measured using optical microscopy is denoted by vertical dashed lines. It is seen that the strain rate sensitivities of the oxidized surfaces are notably higher than those of the unoxidized interiors. The results are independent of the choice of initial focus location and therefore of sample surface topography, consistent with the observations obtained from previous static indentation experiments [10]. The higher average strain rate sensitivity in surface layer implies that the oxidized resin has a limited ductility and thus a greater potential for fracture. This is mostly due to chemical changes that occurred during oxidation including chemical bond breakage and outgassing of low-molecular weight species. It is noticed that the strain rate sensitivities within the oxidized layer are approximately the same, indicating that the microstructure of this oxidized layer is mostly homogeneous. This has been considered to be due to a zero-order reaction [5, 9].

For comparative purpose, the spatial variability of elastic modulus across the oxidized layer is also presented (Figs. 8c and 9c). The static nanoindentation experiments were performed using the "held-at-the-peak" method, a procedure used for testing viscoelastic materials. That is, the indenter was first loaded into the specimen and then held at the maximum load for a certain length of time prior to unloading. The purpose of this procedure was to reduce the viscoelastic effect on indentation unloading response so that the correct elastic stiffness could be calculated. It is seen that the average

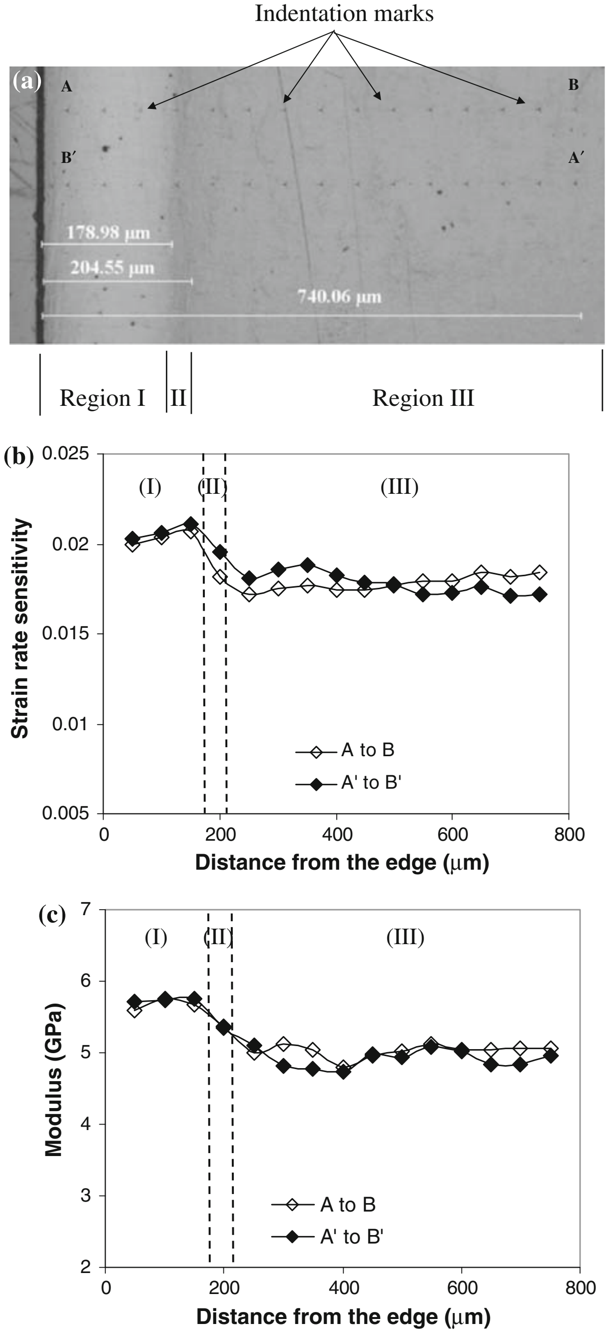

Fig. 8 Spatial variability of mechanical properties of the oxidized PMR-15 aged at 288 °C for 651 h in 0.414-MPa pressurized air. The data were obtained by scan-indenting the oxidized–unoxidized regions by focusing on different locations. **a** Photograph of indented specimen cross section, **b** variation of strain rate sensitivity, and **c** variation of modulus. The *dashed lines* indicate the "transition zone" measured using optical microscopy

modulus in the oxidized region is higher than that in the unoxidized interior, consistent with the strain rate sensitivity results.

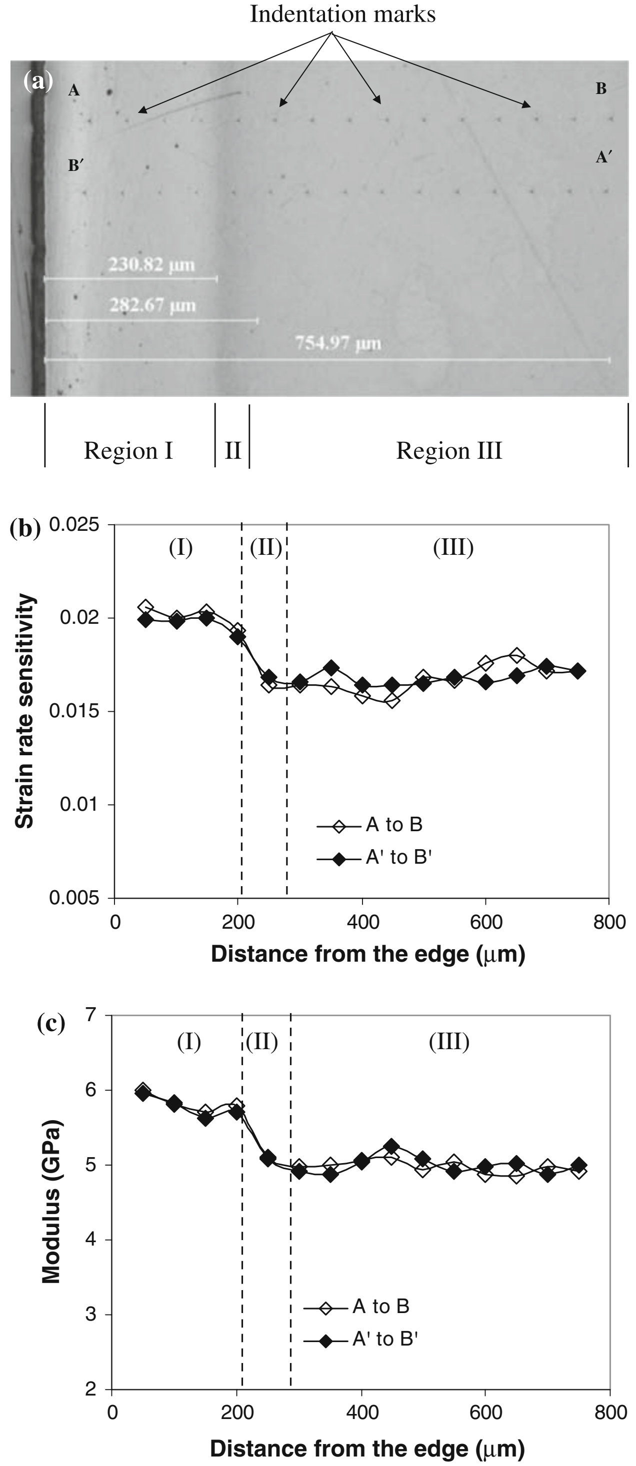

Fig. 9 Spatial variability of mechanical properties of the oxidized PMR-15 aged at 288 °C for 1518 h in 0.414-MPa pressurized air. The data were obtained by scan-indenting the oxidized–unoxidized regions by focusing on different locations. **a** Photograph of indented specimen cross section, **b** variation of strain rate sensitivity, and **c** variation of modulus. The dashed lines indicate the "transition zone" measured using optical microscopy

Effects of environmental conditions on mechanical properties

As discussed in section "Phenomenology of thermo-oxidization of PMR-15", the oxidative profiles of PMR-15 resin specimens are dependent on environmental conditions (time, temperature, and pressure). Longer aging time, higher aging temperature, or higher aging pressure, can result in thicker oxidized surface layer, although the rapid increase generally occurs in the beginning of the oxidation process. The effects of environmental conditions on static mechanical property have been previously studied using nanoindentation [9, 10]. It is found that after passing the initial aging stage, the elastic modulus in the oxidized region becomes relatively insensitive to variations in aging time, temperature, and pressure.

The effects of environmental variables on rate-dependent properties are investigated in this study. Creep tests were performed on specimens with various aging times, temperatures, and pressures. Indentations were performed on the oxidized layer and unoxidized interior, respectively. A total of 15 measurements were made in each region and the average was reported. Figure 10 shows the effect of aging time on strain rate sensitivity of PMR-15 aged at 288 °C. The strain rate sensitivity of the oxidized materials increases rapidly in the beginning of aging and then becomes relatively stable for longer aging-time periods. This is because over time the oxidation occurs at a much lower rate [1–3]. Figure 11 compares the strain rate sensitivity of the specimens isothermally aged at 288, 316, and 343 °C. Results show that the strain rate sensitivities of the oxidized materials are consistently higher than those of the unoxidized interiors. Figure 12 compares the strain rate sensitivity of the PMR-15 specimens isothermally aged at 288 °C in a chamber with (a) ambient pressure, (b) 0.414 MPa pressure, and (c) 0.62 MPa pressure. Similar to other environmental factors, the aging pressure has accelerated the growth of oxidized surface layer since the rate of diffusion of oxygen into the polymer is increased. But once the polymer is fully oxidized (after the initial oxidation stage), the change in mechanical properties remains at a minimum. Overall, the environmental conditions have the similar effect on strain rate sensitivity as they do on rate-independent property (elastic modulus) as reported earlier [10].

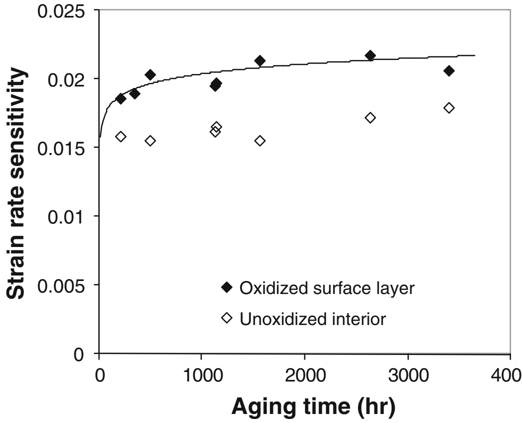

Fig. 10 Effect of the oxidation time on strain rate sensitivity of PMR-15. Specimens used are isothermally aged at 288 °C at lab air condition

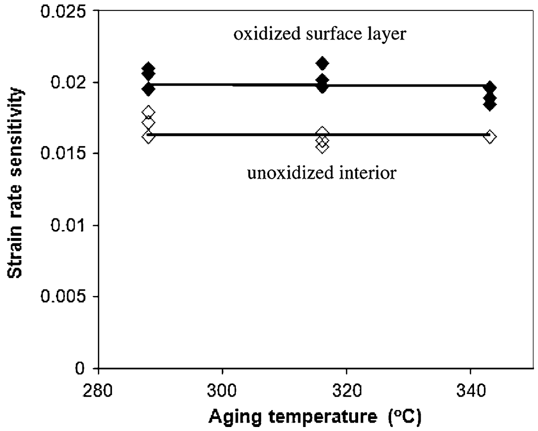

Fig. 11 Effect of the oxidation pressure on strain rate sensitivity of PMR-15. The aging temperatures are 288, 316, and 343 °C

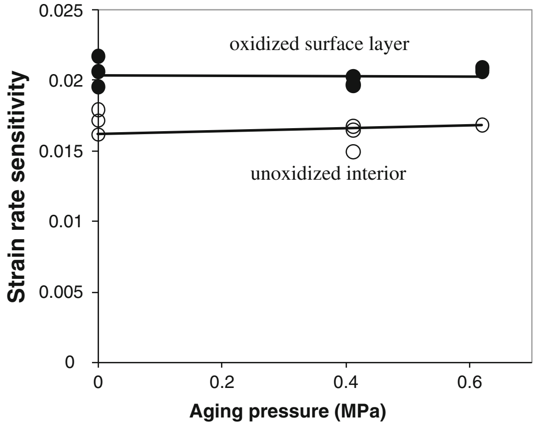

Fig. 12 Effect of the oxidation temperature on strain rate sensitivity of PMR-15. Specimens used are isothermally aged at 288 °C in a chamber with **a** ambient pressure, **b** 0.414 MPa pressure, and **c** 0.62 MPa pressure

Conclusions

The strain rate sensitivity of the oxidized PMR-15 polyimide resin has been successfully determined from nanoindentation creep experiments using a Berkovich indenter. The constant displacement-rate $\left(\dot{h}\right)$ method has been used, in which the histories of hardness and strain rate are monitored. The plot of $\ln(H)$ versus $\ln\left(\dot{h}/h\right)$ has allowed the calculation of strain rate sensitivity. The strain rate sensitivity does not seem to vary with the loading rate used in these creep experiments. The spatial variability of strain rate sensitivity has been examined on specimens oxidized at various environmental conditions (time, temperature, and pressure). In all the cases, the strain rate sensitivity of the oxidized material has been notably higher than that of the unoxidized one. Higher strain rate sensitivity in surface layer implies that the oxidized resin exhibits limited ductility and a potential for fracture. The effect of environmental conditions has been examined on various aged samples. Results show that after a material is fully oxidized (passing the initial oxidative period), the strain rate sensitivity is not much influenced by the environmental conditions.

The mechanical properties of thermal-oxidized polymer resins have been traditionally studied by testing macroscopic tests on bulk specimens, in which the volume of the oxidized layer is only a fraction of the unoxidized core. So the properties of oxidized materials cannot be truly characterized. This study has been the first to examine the rate-dependent deformation of thermal-oxidized PMC resin by performing nano-mechanical tests. It has shown potential for utilizing nanoindentation as a tool to study rate-dependent and rate-independent mechanical deformation of oxidized polymers and composites.

Acknowledgements This study was partially supported by ASEE—Summer Faculty Fellowship Program and performed under the direction of Dr. Greg A. Schoeppner of the Air Force Research Laboratory (AFRL), WPAFB. Y. C. Lu also acknowledges the support obtained from a Kentucky EPSCoR NLI grant.

References

1. Tandon GP, Pochiraju KV, Schoeppner GA (2006) Polym Degrad Stab 91:1861
2. Pochiraju KV, Tandon GP (2006) J Eng Mater Technol 128:107
3. Schoeppner GA, Tandon GP, Pochiraju KV (2007) In: Kwon Y, Allen DH,Talreja R (eds) Multiscale modeling and simulation of composite materials and structures. Springer-Verlag
4. Regnier N, Berriot J, Lafontaine E, Mortaigne B (2001) Polym Degrad Stab 73:485
5. Meadors MA, Lowell CE, Cavano PJ, Herrera-Fierro P (1996) High Perform Polym 8:363
6. Meador MA, Johnston JC, Cavano PJ, Frimer A (1997) Macromolecules 30:3215
7. Meador MA, Johnston JC, Frimer AA, Gilinsky-Sharon P (1999) Macromolecules 32:5532
8. McManus HL, Cunningham RA (1995) Coupled materials and mechanics analyses of durability tests for high temperature polymer matrix composites. NASA/CR-95-112619
9. Johnson LL, Eby RK, Meador MAB (2003) Polymer 44:187
10. Putthanarat S, Tandon GP, Schoeppner GA (2008) J Mater Sci. doi:10.1007/s10853-008-2800-1
11. Putthanarat S, Tandon GP, Schoeppner GA (2007) Polym Degrad Stab 92:2110
12. Schoeppner GA, Curliss DB (2002) Proceedings of the 9th AIAA/ISSMO symposium on multidisciplinary analysis and optimization conference, Atlanta, GA, 4–6 September 2002, AIAA-2002-5516
13. Pollock HM, Maugis D, Barquins M (1986) In: Blau PJ, Lawn BR (eds) Microindentation techniques in materials science and engineering. ASTM, Philadelphia, PA, p 47
14. Mayo MJ, Siegel RW, Liao YX, Nix WD (1992) J Mater Res 7:973
15. Mayo MJ, Siegel RW, Narayanasamy A, Nix WD (1990) J Mater Res 5:1073
16. Mayo MJ, Nix WD (1988) Acta Metall 36:2183
17. Mayo MJ, Nix WD (1988) In: Kettunen PO, Lepisto TK, Lehtonen ME (eds) Strength of metals and alloys. Pergamon Press, Elms ford, NY, p 1415
18. Poisl WH, Oliver WC, Fabes BD (1995) J Mater Res 10:2024
19. Stone DS, Yoder KB (1994) J Mater Res 9:2524
20. Lucas BN, Oliver WC (1999) Metall Mater Trans A 30A:601
21. Cheng Y-T, Cheng C-M (2001) Philos Mag Lett 81:9
22. Bowles KJ, Jayne D, Leonhardt TA (1993) SAMPE Q 24(2):2
23. Bowles KJ, Papadopoulos DS, Inghram LL, McCorkle LS, Klan OV (2001) Longtime durability of PMR-15 matrix polymer at 204, 260, 288 and 316 °C. NASA/TM-2001-210602
24. Tsuji LC, McManus HL, Bowles KJ (1998) Mechanical properties of degraded PMR-15 resin. NASA technical report 1998-208487, p 1
25. Ripberger E, Tandon GP, Schoeppner GA (2004) Proceedings of the SAMPE 2004 symposium/exhibition, Long Beach, CA, 16–20 May 2004 [ITAR restricted]
26. Doerner MF, Nix WD (1986) J Mater Res 4:601
27. Oliver WC, Pharr GM (1992) J Mater Res 7:1564